Optimizing InGaN Heterostructures for High Biosensitivity: Simulations Versus Experiments

Martin F. Schneidereit and Dominik Heinz

In this work, the optimisation of indium gallium nitride (InGaN) heterostructures towards high biosensitivity is presented. Potential changes on the surface of InGaN heterostructures lead to a shift in wavelength and intensity of the photoluminescence (PL) signal of an InGaN quantum well (QW) positioned close to the surface. The semiconductor software nextnano is used to simulate various parameters to find the ideal background doping, QW position and thickness. For live sensing experiments, a new setup with horizontal sample positioning is introduced to enable reproducible verification of the simulation results.

1. Introduction

Gallium nitride (GaN) is widely known for its use in LEDs and, more recently, in high-electron mobility transistors (HEMTs) [1, 2]. With its chemical inertness and stability it is ideal for the use in biological and chemically harsh surroundings [3–6]. The photoluminescence (PL) signal of InGaN quantum well (QW) heterostructures is sensitive to electrical fields within the QW such, that a wavelength emission shift as well as an intensity change can be observed for varying fields present in the QW (quantum-confined Stark effect, QCSE). This effect can be used to detect surface potential changes (compare Fig. 1): due to near-surface band bending, surface potential changes induce electric fields within a QW located close to the surface. Due to this field, wavefunctions from both electrons and holes get more separated for higher internal fields and show reduced separation for lower internal fields. The separation on one hand determines the overlap and thus recombination probability/PL intensity of the exciton. On the other hand, both electrons and holes have their effective recombination energy decreased for higher separation. The surface potential change is thus translated into a PL wavelength shift. It has been shown by several groups (including our own) that InGaN heterostructures can be used for sensing [5, 7, 8].

In order to achieve a maximum response from the QW structure, various sample parameters can be changed and thus optimized. To reduce time and cost for such growth series, simulations are performed with nextnano.

2. Experimental Setup

In order to obtain an undisturbed read-out signal, backside excitation through the substrate is essential. Double-side polished (DSP) sapphire wafers are thus used for the epitaxy of the heterostructures. The setup described in the following can be seen in Fig. 2:

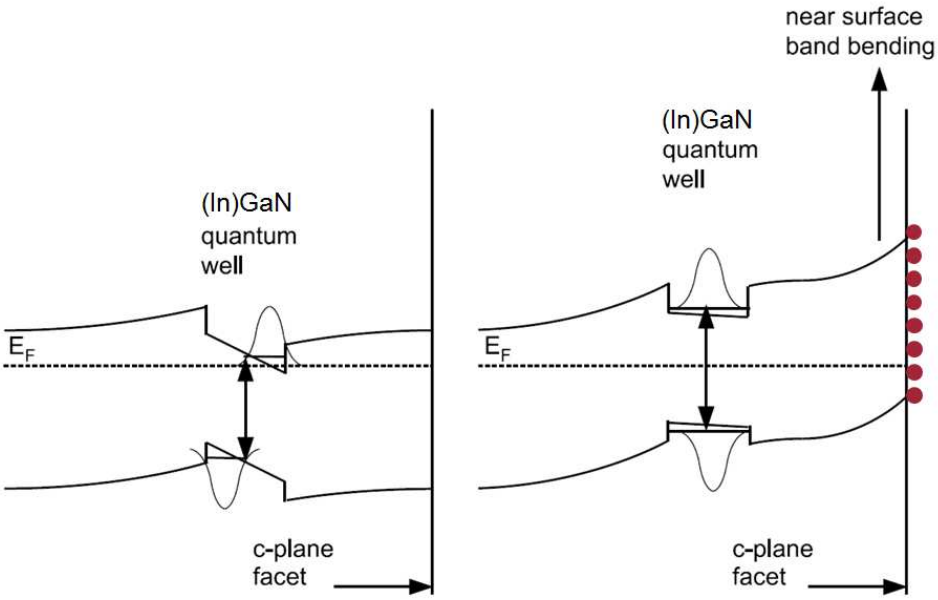

Fig. 1: Sensor principle schematic: for an undisturbed/virgin surface (left), the surface potential is only tilted due to the piezofield of the QW. For adsorbed molecules, the surface potential is shifted (right), resulting in a near-surface band bending which leads to shift in the effective QW recombination energy: surface potential change is translated into QW emission shift.

for live sensing, the sample surface should be horizontal in order to enable application of liquids from the top. In order to measure the spectral shift directly, the spectrum of the QW with an untreated surface is recorded. Then, the molecules are added to the surface via a pipette and the shifted spectrum is recorded. This is done in order to eliminate spectral changes due to inhomogeneities of the heterostructure itself. From the relative position of the peaks, the wavelength shift in nm can be determined, all spectra are normalized for better comparability. To exclude (complete) laser absorption within the GaN bulk material and to excite only the QW, a 405 nm laser is used which has its energy below the bandgap of GaN. The laser beam is coupled into the beamline of the optical setup via a dicroic beamsplitter which reflects the laser but transmits the PL signal. The transmission spectrum of the filter can be seen in the inset of Fig. 2. The beam is then focussed onto the InGaN heterostructure to excite the QW. The PL signal is collected and collimated by the same lens located below the sample. This is done to keep the top side free for adding of sensing liquids. The collimated PL signal is transmitted through the beamsplitter and then reflected by a silver mirror to be focused into the spectrometer unit.

3. Simulation with nextnano

The heterostructures which are grown by metalorganic vapor phase epitaxy (MOVPE) have to be optimized for optical sensing. To maximize the spectral shift originating from the QCSE, various parameters can be adjusted, including: QW thickness, cap layer

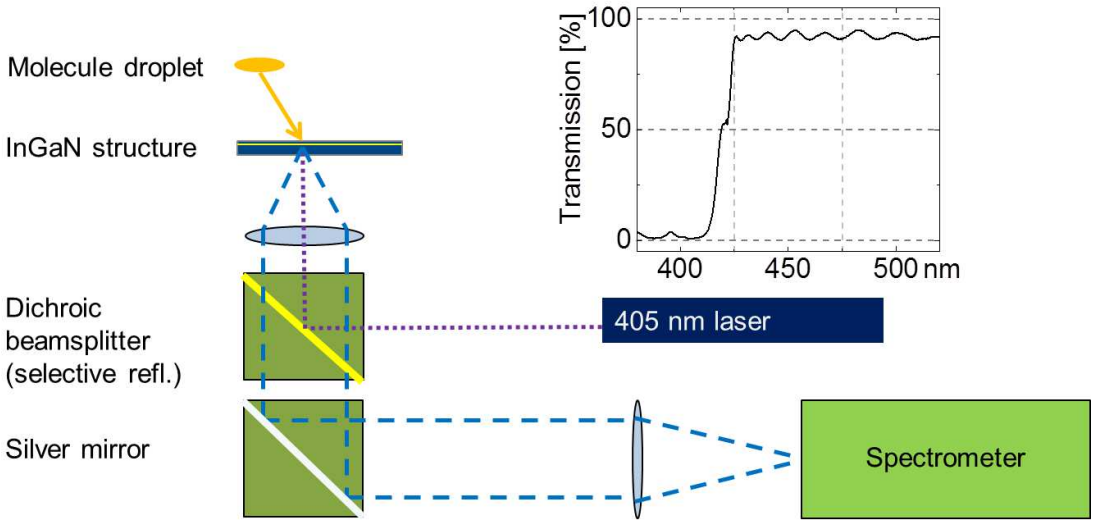

Fig. 2: The setup for live sensing experiments. The beam of a 405 nm laser is coupled into the optical readout beam line via a dichroic beamsplitter (transmission spectrum, see inset) and then focussed onto the InGaN structure from the backside. The PL signal is then also collected from the backside and passes the dichroic filter where it gets reflected by a silver mirror. The collimated signal is then focussed into a spectrometer unit. In order to perform live sensing, a PL spectrum of the structure is recorded and subsequently the test substance is added from the top. The PL emission shift can then be directly observed.

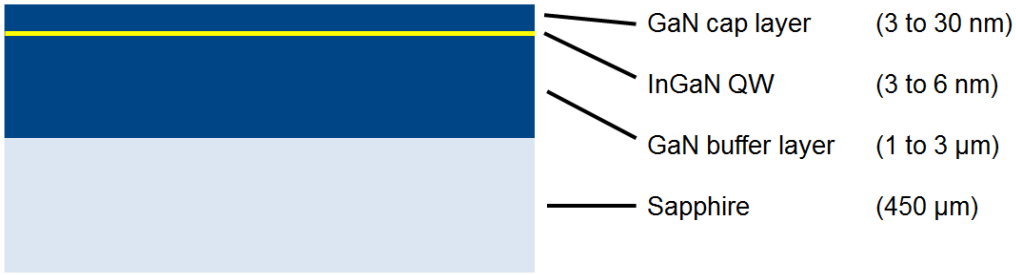

Fig. 3: Schematic of a standard QW heterostructure. The GaN buffer layer (thickness 1–3 µm) is grown on a sapphire substrate of 450 µm. On the buffer layer, a 3–6 nm InGaN layer is grown, which is followed by a GaN cap layer of 3–30 nm. The InGaN embedded between the GaN layers forms the quantum well.

thickness, background doping concentration, indium concentration within the QW (see Fig. 3 for reference). The tool used for these simulations is nextnano, which is an advanced semiconductor device simulation program. nextnano performs a self-consistent solution of Poisson, Schrödinger and drift-diffusion current equations.

As a first means, the QW thickness was varied from 3 nm up to 6 nm in steps of 0.5 nm for different background doping concentrations. It is expected that for a thicker quantum well, the overall potential difference in the QW increases and thus leads to an increased QCSE. This in turn increases the wavelength shift and thus the sensitivity for the given heterostructure. The results are indicated in Fig. 4. With larger thickness, an increased

wavelength shift could be observed from a predefined surface potential shift. The potential shift was chosen to be 0.6 eV as this is the order of magnitude that can be expected from biomolecules. With increasing thickness however, the separation between electron and hole wavefunctions increases linearly, thus reducing their overlap exponentially. This leads to a reduced recombination rate by up to a factor of ≈ 1000. This means that a trade-off has to be met between sensitivity (i.e., the amount of wavelength shift) on one hand and signal intensity, which is related to the recombination rate, on the other. For intermediate thicknesses, high background doping concentrations seem to be desirable.

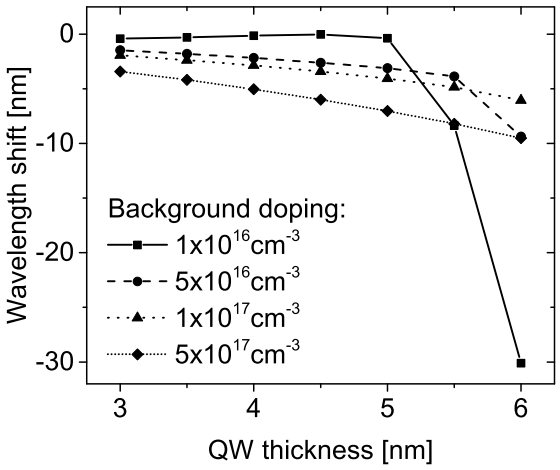

Fig. 4: Wavelength shift versus QW thickness. The dotted curves represent different n-doping concentrations: for higher doping, even thin QWs exhibit an increased shift.

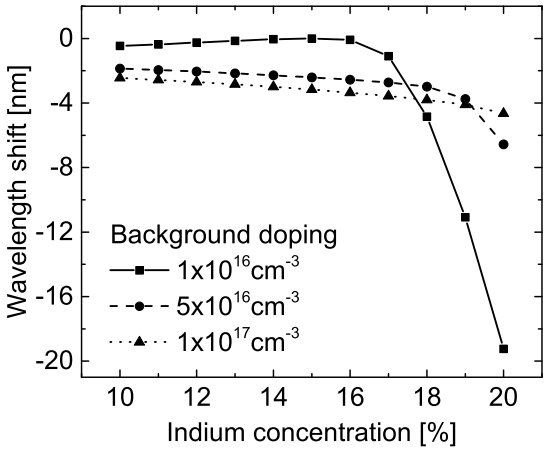

Fig. 5: Wavelength shift versus indium content in the QW. The dotted curves represent different n-doping concentrations: higher doping increases the shift for even low indium content.

The second parameter varied in the simulations was the indium content in the InGaN QWs, again with various background doping concentrations. Considerations were the same as for the QW thickness: with higher indium concentration, strain is increased, as is the QCSE. The simulations confirm these expectations: higher indium concentration leads to a considerably increased sensitivity for low background doping, while for higher doping, the effect is not as prominent (see Fig. 5). The drawback of high indium concentrations (similar to higher QW thicknesses) is that the wavefunction separation increases and leads to reduced signal intensity. For intermediate indium content, again, higher background doping seems to be desirable.

The last parameter that was considered is the positioning of the QW within the GaN bulk, i.e., its position relative to the surface. The barrier between the surface and the QW is called the cap layer. The sensor principle is based on the change of the QCSE which is induced by free carriers within the material. Depending on the background doping, the penetration of the surface band bending into the material happens within few to several hundreds of nanometers. From first considerations done in [9], the higher the field in the QW, the more sensitive it reacts to small potential changes. In the simulations performed, the trend is perfectly clear: highest sensitivity is achieved for QWs positioned close to the surface and for the maximum local field, high doping is needed (see Fig. 7). This matches

well with the previous considerations of higher background doping being advantageous for higher sensitivity. The simulations for 3 nm showed numerical problems and were not included in Fig. 7.

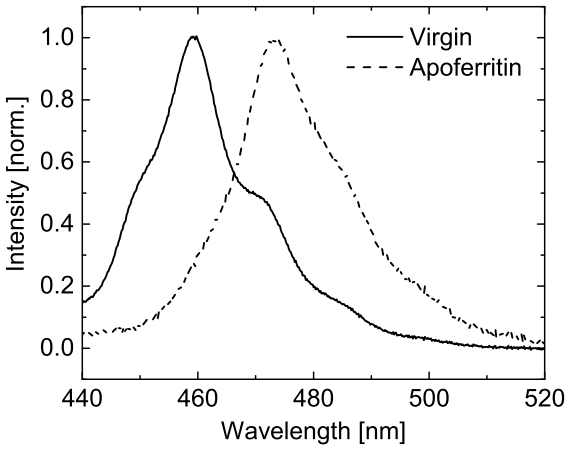

Fig. 6: Representative PL spectra for apoferritin: the virgin surface PL signal was undergoing a red-shift when apoferritin (solved in DI water) was added on top. The observed red-shift was 17 nm for a QW thickness of 3 nm and a cap layer of 3 nm.

4. Comparison Between Simulations and Measurements

With the setup described above, live measurements are possible and thus, first results could be obtained from sensing in liquid environments. As examplary biomolecules, solutions of ferritin and apoferritin[2] have been prepared by S. Chakrabortty et al.[3]. Ferritin is a macromolecule related to the iron household of the human body. Within its hollow core, it can store Fe^{2+} ions and release them at a desired position within the bloodstream [10]. The ferritin concentration in the blood is an indicator for various health conditions, such as chronic anemia [11]. With our sensor structure we want to detect the iron content of ferritin itself, which is expected to be an even superior biomarker for further diseases such as Alzheimer's disease [12]. For first analysis, the influence of the biosolvent on the surface potential was investigated. The intrinsic wavelength shift of the biosolvent has to be taken into account for an exact determination of the molecule's concentration later on. The shift is determined by analyzing and comparing the spectra of the virgin surface versus the surface with added molecules/liquids. An exemplary apoferritin analysis can be seen in Fig. 6. While deionized (DI) water did not show any spectral shift, toluene showed a spectral shift of 4.4 nm (both see Fig. 9). DI water is used as solved for pure ferritin and apoferritin, while toluene is used for later stages of the experiments.

The next step was to analyze the molecules themselves (see Fig. 10): ferritin and apoferritin were analyzed for different cap layer thicknesses[4] to compare with the results

[2]Apoferritin is ferritin depleted of iron.
[3]Institute of Organic Chemistry III, Ulm University
[4]Samples with cap layers > 9 nm had faulty growth runs and could not be investigated.

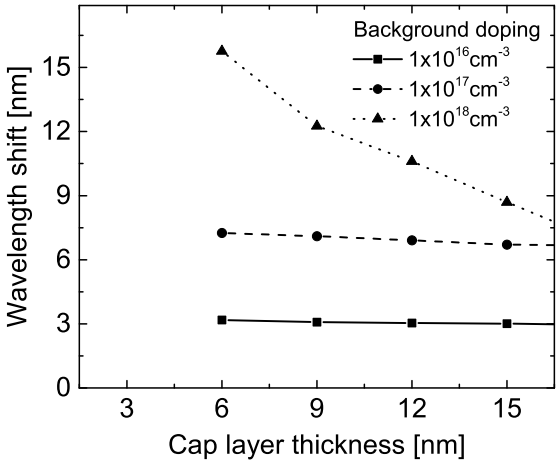

Fig. 7: Wavelength shift vs. cap layer thickness for various doping concentrations. Thin cap layers show the strongest shift and with high doping, the response maximizes.

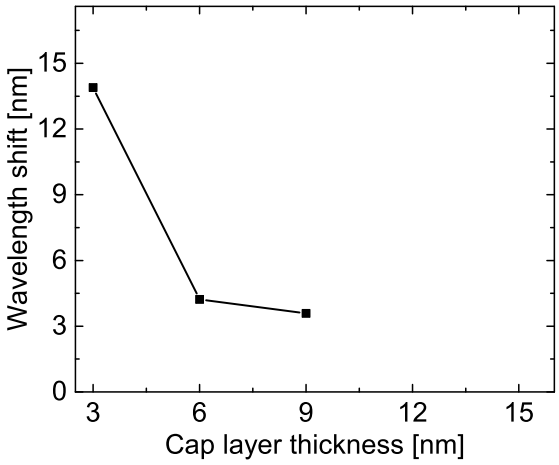

Fig. 8: Measurements of three samples with different cap layer thicknesses. From the simulations the doping concentration is concluded to be around $0.5 \cdot 10^{17}\mathrm{cm}^{-3}$.

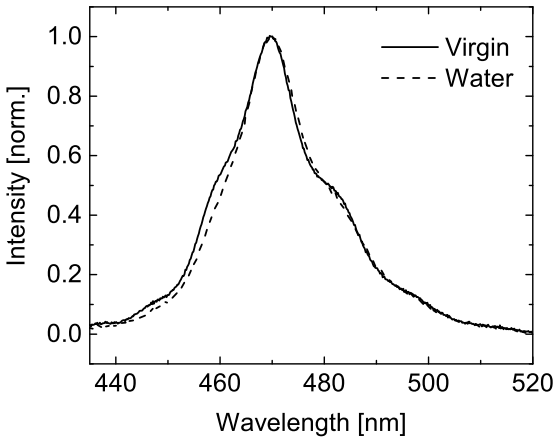

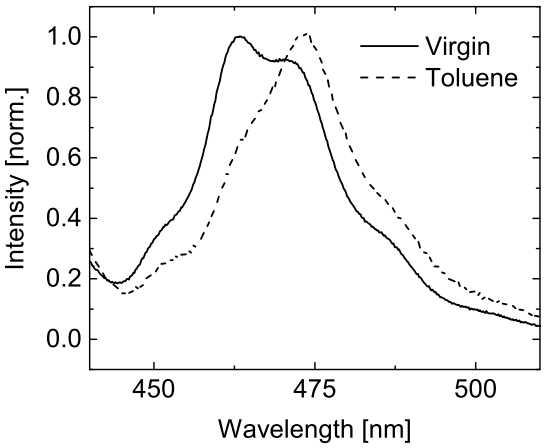

Fig. 9: Spectral shifts of biosolvents: DI water (left) did not lead to any spectral shift of the PL signal. For toluene (right), a spectral red-shift of 4.4 nm can be observed.

discussed in Sect. 3. The results were mostly as expected: for the thinnest cap layer, the sensing shift was highest, whereas for thicker cap layers the shift reduced (see Fig. 8). When compared to the simulations in detail, the results point to a background doping concentration of $\approx 0.5 \cdot 10^{17}\mathrm{cm}^{-3}$, which is reasonable for MOVPE growth with unintended background doping from contaminants. In order to better determine the shift in surface potential due to the adsorption of apoferritin, the simulations were used to approach the observed shift by assuming various surface potential changes. The results can be seen in Fig. 11: due to the observed wavelength shift, a surface potential change of $-1.6\,\mathrm{eV}$ is concluded. This is higher than expected, errors might arise from donor concentration which was assumed to be $\approx 1 \cdot 10^{16}\mathrm{cm}^{-3}$ but is possibly higher (compare results above). All in all, the simulations match well with the expected result, even though uncertainties remain about exact surface starting potential and induced shift by the biomolecules.

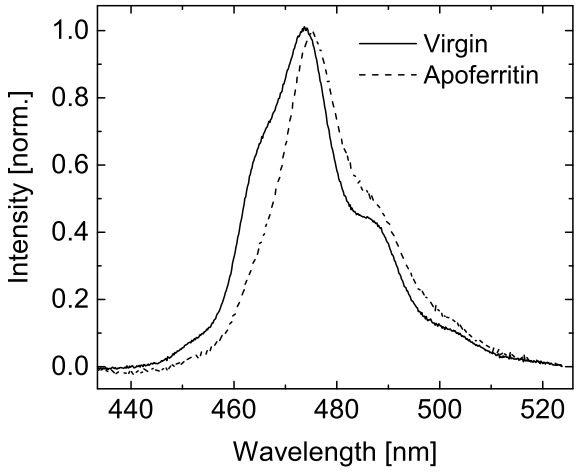

Fig. 10: Comparison between measurement and simulation for apoferritin sensing: the observed red-shift was 3.5 nm for a QW thickness of 3 nm and a cap layer of 9 nm.

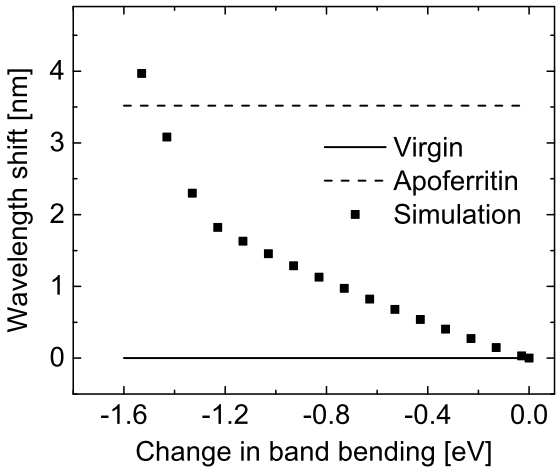

Fig. 11: QW simulations for Fig. 10: for the given sample, the surface potential was changed and the resulting wavelength shift was compared to the measurement. The matching potential change was −1.6 eV.

5. Summary

In conclusion, a setup for horizontal excitation is demonstrated, enabling live sensing experiments on fixed sample positions. These live sensing results are used to better understand the sensing behaviour of InGaN QW heterostructures and to confirm the results found in [7]. They are also compared to the simulations done in nextnano, which have been performed in order to optimize the heterostructure design parameters to achieve maximum biosensitivity. With both, simulations and experiments, further QW samples will be improved to come closer to our final goal of realising medical sensors for biomolecules.

Acknowledgment

Scientifc support by J. Shabaz (Institute of Optoelectronics, Ulm University), F. Huber, S. Bauer, B. Hörbrand, K. Thonke (Institute of Quantum Matter / Semiconductor Physics Group, Ulm University), S. Chakrabortty, N. Naskar and T. Weil (Institute of Organic Chemistry III, Ulm University) is gratefully acknowledged. This work was financially supported by the Baden-Württemberg Stiftung gGmbH within the project: "Intelligente optoelektronische Biosensoren".

References

[1] N. Koide, H. Kato, M. Sassa, S. Yamasaki, K. Manabe, M. Hashimoto, H. Amano, K. Hiramatsu, and I. Akasaki, "Doping of GaN with Si and properties of blue m/i/n/n^+ GaN LED with Si-doped n^+-layer by MOVPE", *J. Cryst. Growth*, vol. 115, pp. 639–642, 1991.

[2] R.S. Pengelly, S.M. Wood, J.W. Milligan, S.T. Sheppard, and W.L. Pribble, "A review of GaN on SiC high electron-mobility power transistors and MMICs", *IEEE Trans. Microw. Theory Techn.*, vol. 60, pp. 1764–1783, 2012.

[3] I. Yonenaga, "Thermo-mechanical stability of wide-bandgap semiconductors: high temperature hardness of SiC, AlN, GaN, ZnO and ZnSe", *Physica B: Condensed Matter*, vol. 308–310, pp. 1150–1152, 2001.

[4] K.-A. Son, A. Liao, G. Lung, M. Gallegos, T. Hatake, R.D. Harris, L.Z. Scheick, and W.D. Smythe, "GaN-based high-temperature and radiation-hard electronics for harsh environments", in *Micro- and Nanotechnology Sensors, Systems, and Applications II*, T. George, M.S. Islam, and A.K. Dutta (Eds.), Proc. SPIE 7679, pp. 76790U-1–8, 2010.

[5] S. Pearton, B. Kang, S. Kim, F. Ren, B. Gila, C. Abernathy, J. Lin, and S. Chu, "GaN-based diodes and transistors for chemical, gas, biological and pressure sensing", *J. Phys. Condens. Mat.*, vol. 16, p. R961–R994, 2004.

[6] I. Cimalla, F. Will, K. Tonisch, M. Niebelschütz, V. Cimalla, V. Lebedev, G. Kittler, M. Himmerlich, S. Krischok, J. Schaefer, M. Gebinoga, A. Schober, T. Friedrich, and O. Ambacher, "AlGaN/GaN biosensor-effect of device processing steps on the surface properties and biocompatibility", *Sens. Actuators B*, vol. 123, pp. 740–748, 2007.

[7] D. Heinz, F. Huber, M. Spiess, M. Asad, L. Wu, O. Rettig, D. Wu, B. Neuschl, S. Bauer, Y. Wu, S. Chakrabortty, N. Hibst, S. Strehle, T. Weil, K. Thonke, and F. Scholz, "GaInN quantum wells as optochemical transducers for chemical sensors and biosensors", *IEEE J. Sel. Topics Quantum Electron.*, vol. 23, pp. 1–9, 2017.

[8] S. Paul, A. Helwig, G. Müller, F. Furtmayr, J. Teubert, and M. Eickhoff, "Optochemical sensor system for the detection of H2 and hydrocarbons based on InGaN/GaN nanowires", *Sens. Actuators B*, vol. 173, pp. 120–126, 2012.

[9] O. Rettig, *Nitridische Nanosäulen – Design und Wachstum für Sensoranwendungen*, Master Thesis, Ulm University, Ulm, Germany, 2014.

[10] Y. Ren and T. Walczyk, "Quantification of ferritin bound iron in human serum using species-specific isotope dilution mass spectrometry", *Metallomics*, vol. 6, pp. 1709–1717, 2014.

[11] G. Weiss and L.T. Goodnough, "Anemia of chronic disease", *N. Engl. J. Med.*, vol. 352, pp. 1011–1023, 2005.

[12] P.D. Sole, C. Rossi, M. Chiarpotto, G. Ciasca, B. Bocca, A. Alimonti, A. Bizzarro, C. Rossi, and C. Masullo, "Possible relationship between Al/ferritin complex and Alzheimer's disease", *Clinical Biochemistry*, vol. 46, pp. 89–93, 2013.